

Iron-accumulating splenocytes may exacerbate non-alcoholic steatohepatitis through the production of proinflammatory cytokines and reactive oxygen species

Kazutoshi Murotomi¹ , Hirosuke Tawara², Mitsuko Sutoh² and Mayu Yasunaga³

¹Biomedical Research Institute, National Institute of Advanced Industrial Science and Technology (AIST), Tsukuba 305-8566, Japan;

²Institute for Animal Reproduction, Kasumigaura 300-0134, Japan; ³Health and Medical Research Institute, National Institute of Advanced Industrial Science and Technology (AIST), Tsukuba 305-8566, Japan

Corresponding author: Kazutoshi Murotomi. Email: k-murotomi@aist.go.jp

Impact Statement

NASH is a manifestation of metabolic syndrome in the liver, and the complex mechanism of NASH development has not been fully elucidated. A significant correlation between splenic iron level and NASH severity was previously reported in TSOD mice, suggesting that the spleen contributes to NASH pathogenesis through the release of splenocyte-derived molecules via the portal vein. In this study, we found that the spleens of mice in the early stage of NASH accumulate iron, and that iron-accumulating splenocytes generate moderate amounts of ROS and release high amounts of TNF- α after macrophage stimulation. Thus, spleen-derived ROS and proinflammatory cytokines may indirectly contribute to hepatic inflammation. These results indicate that iron metabolism modulation in the spleen may contribute to developing novel therapeutic strategies for NASH.

Abstract

Non-alcoholic steatohepatitis (NASH) results from non-alcoholic fatty liver disease (NAFLD) via multiple-parallel events, including hepatic triglyceride accumulation, oxidative stress, and inflammation. The complex interaction between the liver and multiple other organs is involved in NASH development. Although spleen-derived humoral factors can directly contribute to NAFLD/NASH onset via the portal vein, the status of the spleen in the early stage of NASH remains unknown. Here, our aim was to investigate whether splenocytes may exacerbate NASH via the generations of reactive oxygen species (ROS) and proinflammatory cytokines. Iron accumulation was observed in the spleen but not the liver, and the proportion of phagocytic macrophages increased in the spleen of Tsumura Suzuki Obese Diabetes (TSOD) mice showing histological characteristics of NASH in the early stage. The splenocytes generated moderate amounts of ROS and released high amounts of tumor necrosis factor (TNF)- α in response to lipopolysaccharide, indicating excessive inflammatory cytokine released by activated macrophages in iron-accumulating spleens. Our results suggest that iron-accumulating splenocytes can easily induce inflammation and contribute to exacerbate NASH via the portal vein. Thus, the regulation of iron metabolism in the spleen should be considered in the development of novel therapeutic targets against NASH.

Keywords: Iron, spleen, inflammation, reactive oxygen species, non-alcoholic steatohepatitis

Experimental Biology and Medicine 2022; 247: 848–855. DOI: 10.1177/15353702221077218

Introduction

Non-alcoholic fatty liver disease (NAFLD) is a manifestation of metabolic syndrome in the liver, and approximately 25% of NAFLD patients develop non-alcoholic steatohepatitis (NASH), which is characterized by steatosis, lobular inflammation, and fibrosis in the liver. NASH can result in serious and irreversible diseases, including liver cirrhosis and hepatocellular carcinoma.¹ A “two-hit hypothesis” has been used to explain the pathogenesis/progress of NASH, which is based on a first hit consisting of obesity and insulin

resistance-mediated hepatic steatosis, and a second hit consisting of inflammatory cytokines, free radicals, and iron overload, which are required to further exacerbate liver injury.² However, a “multiple-parallel hit hypothesis” has recently been proposed for the development of NAFLD/NASH,³ which is associated with adipose tissue-derived free fatty acid-induced hepatic triglyceride accumulation and lipotoxicity, mitochondrial dysfunction, oxidative stress, endoplasmic reticulum stress, and gut-derived-lipopolysaccharide (LPS)-induced inflammation.^{1,3–6} There is growing evidence that the complex interaction between the liver

and multiple other organs, including the adipose tissue, gut, and brain, contributes to NASH pathogenesis and progression.^{5,7-9}

The spleen modulates the immune system by serving as the main filter for blood-borne pathogens and antigens, and also plays an important role in iron metabolism and erythrocyte homeostasis. It is anatomically linked to the liver via the splenic and portal veins, and spleen-derived humoral factors affect the hepatic state; splenic lipocalin-2 is an anti-microbial protein that enters the liver through the portal vein and regulates hepatic immune tolerance.¹⁰ A splenectomy changes the phenotype of hepatic macrophages during liver fibrosis¹¹ as well as attenuates hepatic fibrosis in diet-induced NASH model rats.¹² We previously showed that iron is accumulated in the spleens of Tsumura Suzuki Obese Diabetes (TSOD) mice, which exhibit histopathological features of NASH and develop slight liver fibrosis and hepatocellular carcinoma.¹³ In addition, we have shown that the iron level in the spleen is positively correlated with the severity of NASH.¹⁴ These findings indicate that the spleen is one of the organs contributing to NASH pathogenesis and progression, and that splenocyte-derived molecules can be directly involved in the pathogenesis of NAFLD/NASH via the portal vein. However, the nature of these molecules in the early stages of NASH remains unclear. This study aimed to determine whether splenocytes may exacerbate NASH via excessive generation of reactive oxygen species (ROS) and proinflammatory cytokines.

Materials and methods

Animal experiments

Four-week-old male TSOD mice and age-matched Tsumura Suzuki Non-Obese (TSNO) control mice were obtained from the Institute for Animal Reproduction (Ibaraki, Japan), housed in cages (three per cage), and provided free access to a standard food (CE-2; Clea Japan Inc., Tokyo, Japan) and water under a temperature of $23 \pm 2^\circ\text{C}$, humidity of $50 \pm 10\%$, and a 12-h light (8:00–20:00) and dark (20:00–8:00) cycle. The animals were allowed to acclimatize to the laboratory environment for a week before experiments. All animals were euthanized at 5 and 12 weeks of age with sevoflurane anesthesia, and the liver and spleen were collected. The study protocol was approved by the Institutional Animal Care and Use Committee of the National Institute of Advanced Industrial Science and Technology.

Measurement of iron levels using inductively coupled plasma mass spectrometry

Iron levels were measured as previously described.¹⁴ In brief, the livers and spleens from TSOD or TSNO mice ($n=6$ each) were lysed using T-PER (Thermo Fisher Scientific Inc., Waltham, MA, USA), followed by digestion of the lysates in HNO_3 and overnight incubation at 25°C . The digested tissues were diluted in ultrapure water and examined by inductively coupled plasma mass spectrometry (ICP-MS) (XSeries II; Thermo Fisher Scientific Inc.). The iron standard solution (Kanto Chemical Co., Inc., Tokyo, Japan) was used

for calibration. Iron levels were compensated for by the protein levels in tissues, which were measured using the BCA protein assay kit (Pierce, IL, USA).

RNA isolation and quantitative real-time polymerase chain reaction

Spleens and livers from TSOD or TSNO mice ($n=6$ each) were preserved with RNeasy Lysis Buffer (Thermo Fisher Scientific Inc.), and total RNA was isolated using RNeasy Mini kit (QIAGEN, Hilden, Germany). Single-stranded cDNA was synthesized using ReverTraAce (TOYOBO, Shiga, Japan). Gene expression was assessed using KOD SYBR quantitative polymerase chain reaction (qPCR) Mix (TOYOBO) and a CFX Connect Real-Time System (Bio-Rad, Hercules, CA, USA). The following primers were used: 5'-GCCTGTCTCCTGCTTCTCTCT-3' and 5'-GCTCTGTAGTCTGTCTCATCTGTT-3' for mouse *Hamp*, 5'-GCTCGAATGAACACTCTGG-3' and 5'-GTTCCTCTGTCAGCATCAC-3' for mouse *Hmox1*, 5'-ACTACA CCGAGATGAACGA-3' and 5'-GACGTACTTGAGGGAA TTCAG-3' for mouse *Gpx1*, and 5'-GTGGAGCCAAAAG GGTCATCATCT-3' and 5'-CCTCCTCAGACCGCTTTTTT-3' for mouse *Gpadh*. The amplification conditions were as follows: 98°C for 2 min, followed by 40 cycles at 98°C for 10 s, 60°C for 10 s, and 68°C for 30 s. The melting curve was analyzed in a linear temperature gradient ($65\text{--}95^\circ\text{C}$) to assess whether a single polymerase chain reaction (PCR) product was synthesized. Relative gene expression levels were determined after normalization to *Gapdh* expression level.

Isolation of splenocytes and ROS measurements

Mouse splenocytes were harvested using our previously reported method.¹⁴ Briefly, tissues from TSOD or TSNO mice ($n=3$ each) were dispersed in ice-cold HBSS (Wako Pure Chemical Industries, Ltd., Osaka, Japan) and centrifuged at 500g for 20 min in 37% Percoll (Sigma-Aldrich Inc., MO, USA). Red blood cell lysis buffer (BioLegend, San Diego, CA, USA) was added to the pellet and incubated on ice. The suspension was centrifuged at 500g for 5 min and the resulting pellet was washed with RPMI medium (Wako Pure Chemical Industries, Ltd.) twice. After the centrifugation, the pellet was resuspended in RPMI and the splenic cells were counted using a countess automated cell counter (Invitrogen, MA, USA).

Isolated splenic cells (5×10^5 cells/well) were seeded into 24-well plates (Thermo Fisher Scientific Inc.). After overnight incubation, the cells were cultured in RPMI medium and treated with or without 1 mM hydrogen peroxide (H_2O_2) for 1 h and incubated with HBSS containing $10 \mu\text{M}$ of 2',7'-dichlorodihydrofluorescein diacetate (DCFH-DA; Sigma-Aldrich Inc.) for 30 min. After washing with PBS, the cells were analyzed by flow cytometry using the FACSCalibur system (Becton Dickinson, Franklin Lakes, NJ, USA).

Measurement of tumor necrosis factor- α levels in the supernatants of cultured splenocytes

Isolated splenocytes (1×10^5 cells/well) from TSOD or TSNO mice ($n=3$ each) were seeded into 96-well plates (Thermo

Fisher Scientific Inc.) and cultured with RPMI overnight. For leukocyte activation, 10 µg/mL LPS or 50 ng/mL phorbol 12-myristate 13-acetate (PMA) + 1 µg/mL ionomycin was added to cultured cells. After 48 h of incubation, tumor necrosis factor (TNF)- α levels were measured in the supernatants using an enzyme-linked immunoassay (ELISA) kit (eBioscience, Inc., CA, USA).

Identification of macrophage subset

The isolated splenocytes from TSOD or TSNO mice ($n=3$ each) were blocked with anti-CD16/CD32 (BD Biosciences, CA, USA), followed by surface staining of CD11b (BioLegend, Cat# 101205, dilution 1:125), F4/80 (BD Biosciences Cat# 565410, dilution 1:125), and CD68 (BioLegend, Cat# 137007, dilution 1:125). An isotype control was used as a negative control for each fluorescent dye. After washing with PBS, the cells were analyzed by flow cytometry.

Statistical analysis

Data are presented as mean values \pm SEs, and the number of replicates in the figure legends represents biological replicates. Statistical analyses were performed using the unpaired Student's *t*-test for two-group comparisons. Analysis of variance followed by Tukey's test was used for multiple comparisons using Ekuseru-Toukei 2012 software (Social Survey Research Information Co., Ltd., Tokyo, Japan) according to the experimental design. $P < 0.05$ was considered significant.

Results

Iron accumulates in the spleen of TSOD mice

We compared hepatic and splenic iron levels between TSOD and control TSNO mice at age 12 weeks. Hepatic iron content was comparable between the two mouse strains (25.7 ± 1.44 and 24.4 ± 1.73 ppb/mg protein in TSNO and TSOD mice, respectively) (Figure 1(a)). However, the splenic iron level in TSOD mice was markedly higher than that in TSNO mice ($11,932.8 \pm 1719.7$ and 508.3 ± 45.3 ppb/mg protein, respectively) (Figure 1(b)). The expression levels of *Hamp*, which encodes a systemic iron homeostasis regulator hepcidin,¹⁵ were significantly increased in the spleen (Figure 1(d)) but not the liver (Figure 1(c)) of TSOD mice compared with those in TSNO mice. These results suggested that iron accumulates in the spleen of TSOD mice showing histological features of NASH in the early stage.

Iron accumulation in splenocytes from TSOD mice induces ROS generation and increased expression of antioxidant genes

The reaction between ferrous iron (Fe^{2+}) and H_2O_2 is termed the Fenton reaction and generates hydroxyl radical ($\text{HO}\cdot$). To investigate whether the accumulation of iron in splenocytes generates excessive ROS, we compared their levels between isolated splenocytes from TSNO and TSOD mice. DCFH-DA fluorescence intensity in splenocytes from TSOD mice was higher than that in splenocytes from TSNO mice, regardless

of whether H_2O_2 was added or not (Figure 2(a)). The percentages of DCFH-DA⁺ cells included in the M1 area in TSNO and TSOD mice were $6.71 \pm 0.59\%$ and $13.57 \pm 0.93\%$, respectively (Figure 2(a)).

Hmox1 and *Gpx1* encode antioxidant enzymes and are upregulated by ROS.¹⁶ Here, their mRNA levels were significantly increased in the spleens of TSOD mice compared to those in TSNO mice (Figure 2(b) and 2(c)), indicating that iron accumulation in the splenocytes of TSOD mice promotes ROS generation, but that this excessive ROS generation may be attenuated by increasing the expression of antioxidant enzymes.

Iron accumulation in the spleen is accompanied by excessive TNF- α production upon macrophage activation

Since intracellular iron promotes the production of inflammatory cytokines,¹⁷ we examined TNF- α production by splenocytes. TNF- α levels in non-stimulated splenocytes (control) were undetectable (Figure 3). When the splenocytes were treated with PMA and ionomycin for T-cell stimulation, TNF- α levels in the supernatants were higher than those in the control, but the levels were almost the same between TSNO (345.6 ± 60.0 pg/mL) and TSOD (271.7 ± 18.1 pg/mL) splenocytes. In contrast, TNF- α levels in the supernatants of TSOD splenocytes were significantly higher than those in the supernatants of TSNO splenocytes (1257.4 ± 93.3 and 433.0 ± 62.9 pg/mL, respectively) after macrophage stimulation with LPS (Figure 3).

Macrophages in splenic red pulps reportedly phagocytize senescent and damaged erythrocytes to recycle iron.¹⁸ To identify the subset of macrophages that is localized in iron-accumulating spleens at the early stage of NASH, we measured the distribution of the macrophage marker F4/80, which is typically considered a mature macrophage marker,¹⁹ and CD68, which is a marker associated with macrophage activation.²⁰ The percentage of F4/80⁺CD68⁺ macrophages was higher in TSOD splenocytes than in TSNO splenocytes (Figure 4(a) to (c)). In addition, the percentage of F4/80-CD68⁺ macrophages was similar between TSNO and TSOD splenocytes at age 5 weeks (Figure 4(a) and (d)), whereas the percentage at age 12 weeks was markedly higher in TSOD splenocytes than in TSNO splenocytes ($7.7 \pm 2.2\%$ vs $1.2 \pm 0.2\%$; Figure 4(b) and (d)). These results indicated that iron accumulation in the spleen is accompanied by increases in the proportion of immature and activated macrophages with phagocytic activity. Moreover, the results indicated that excessive amounts of TNF- α are released upon macrophage activation in the spleens of TSOD mice, and that non-stimulated splenocytes in TSOD mice release only a small amount of TNF- α .

Discussion

We previously observed the accumulation of hemosiderin, an iron-storage complex in macrophages, in the spleen of TSOD mice at age 12 weeks and detected a significant correlation between splenic iron level and NASH severity.¹⁴

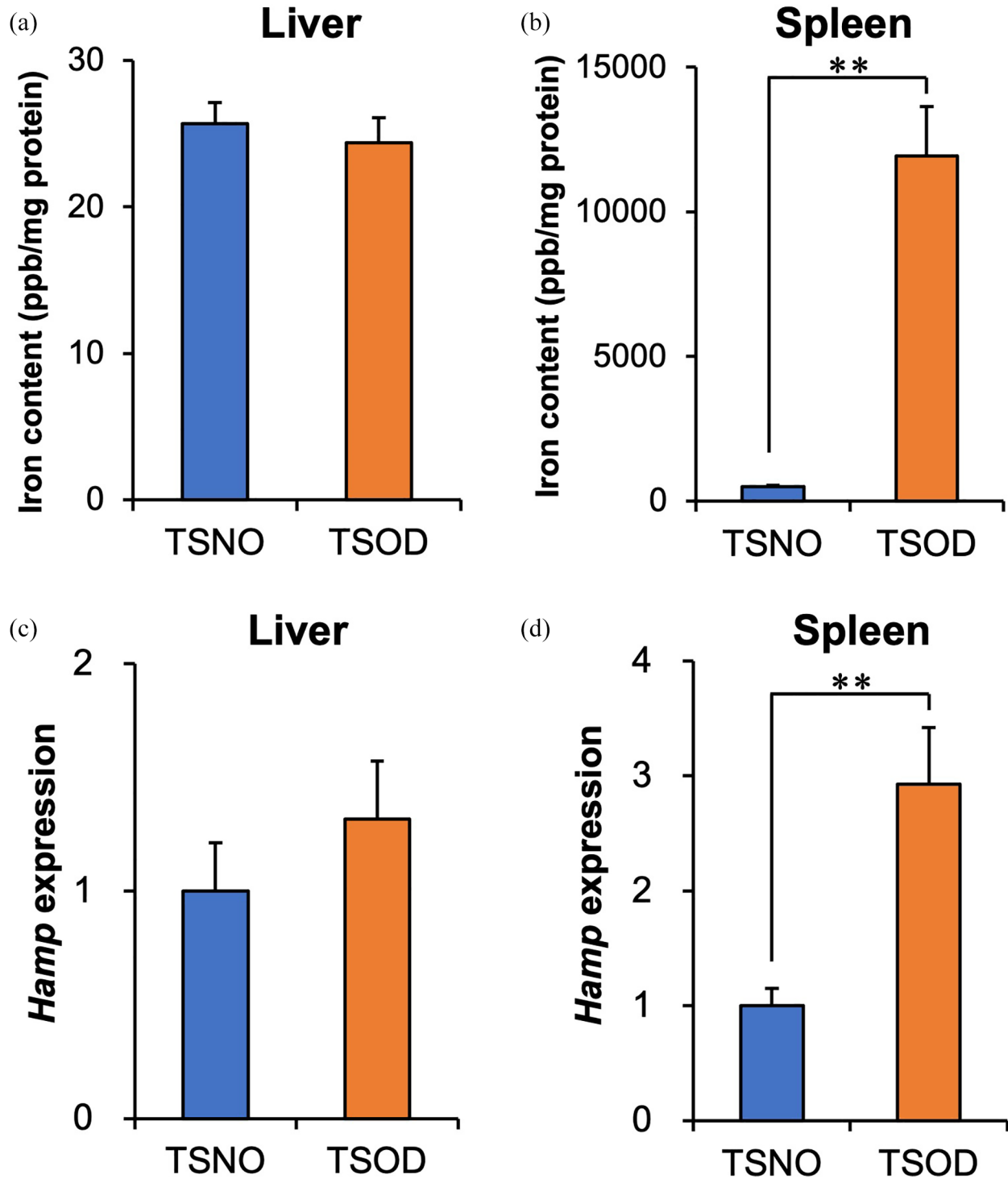


Figure 1. Hepatic and splenic iron levels in TSNO and TSOD mice. Iron levels in the liver (a) and spleen (b) as determined by ICP-MS. An iron standard solution was used as reference and adjusted by the protein level in the tissues. Data are presented as the mean values \pm SE ($n=6$ each). The expression levels of *Hamp* in the liver (c) and spleen (d) as determined by qPCR. Data are presented as mean values relative to TSNO \pm SE ($n=6$ each). (A color version of this figure is available in the online journal.)

** $P < 0.01$ compared with TSNO.

These findings suggested that the spleen contributes to NASH pathogenesis and progression through the release of splenocyte-derived molecules via the portal vein. However, the nature of these molecules remained unclear. Here, we

sought to investigate whether splenocytes may exacerbate NASH through ROS and proinflammatory cytokine production. We observed iron accumulation in the spleens, but not the livers, of TSOD mice exhibiting NASH at an

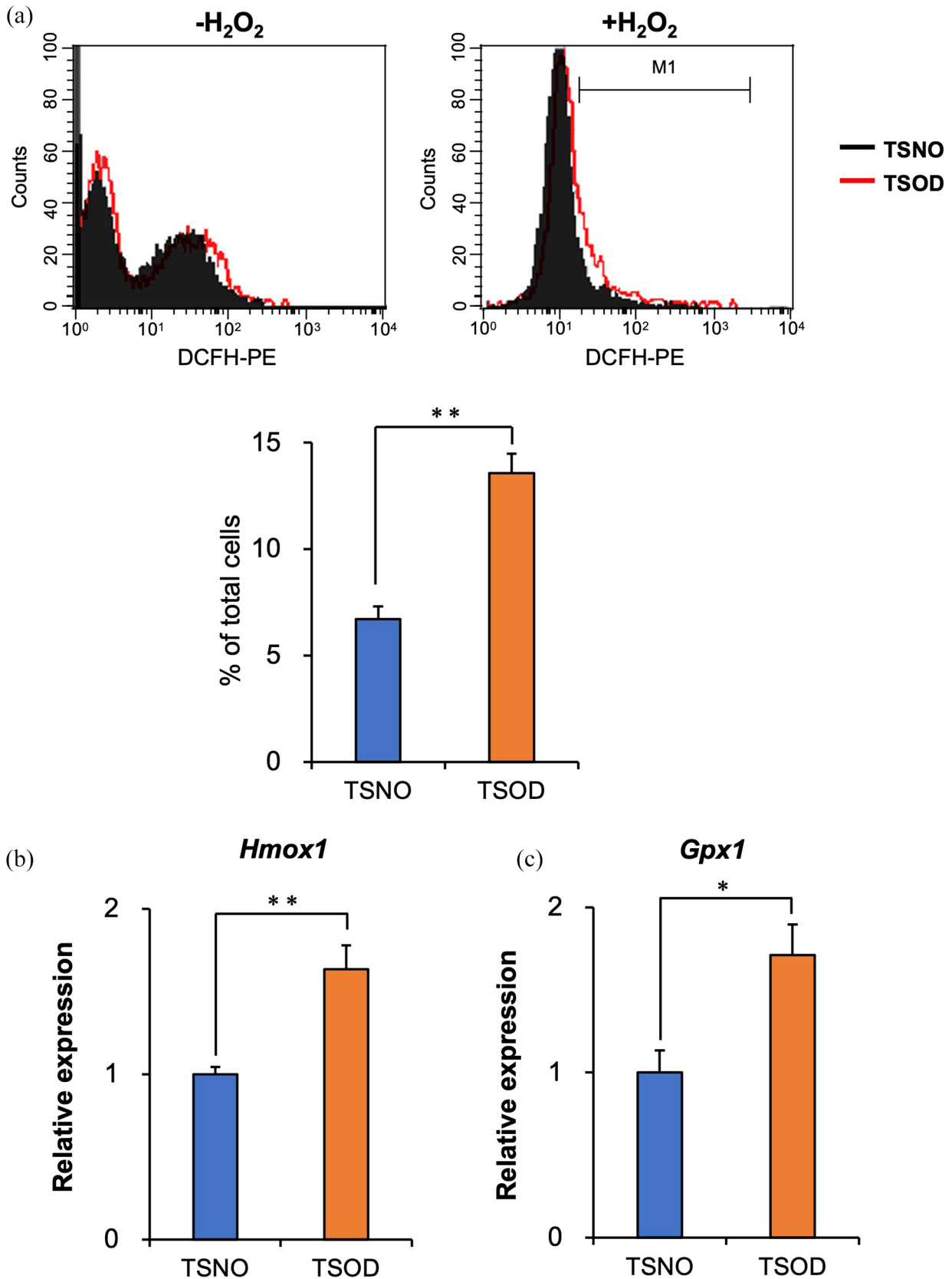


Figure 2. ROS generation and expression of antioxidant genes. (a) Differences in the fluorescence intensity of DCFH-DA in splenocytes of TSNO and TSOD mice with and without H₂O₂. The bar graph indicates the percentage of cells in the M1 range after H₂O₂ treatment. *Hmox1* (b) and *Gpx1* (c) expression levels determined after normalization to the expression level of *Gapdh*. Data are presented as the mean values ± SE (*n*=6 each). (A color version of this figure is available in the online journal.) **P* < 0.05; ***P* < 0.01 compared with TSNO.

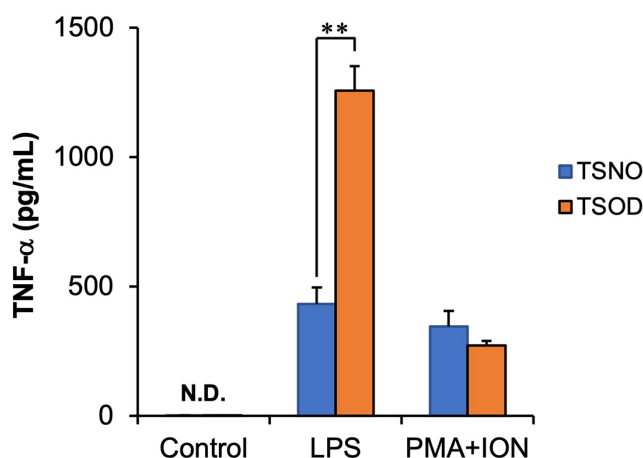


Figure 3. TNF- α levels in the supernatants of cultured splenocytes from TSNO and TSOD mice. Splenocytes from TSNO and TSOD mice were seeded into 96-well plates and TNF- α concentration in the supernatants was determined using an ELISA kit. (A color version of this figure is available in the online journal.)

LPS: lipopolysaccharide; PMA: phorbol 12-myristate 13-acetate; ION: ionomycin. Data are presented as the mean values \pm SE ($n=3$ each).

** $P < 0.01$ compared with TSNO.

early stage (Figure 1(a) and (b)), consistent with our previous findings. Furthermore, we found that iron-accumulating splenocytes could generate moderate amounts of ROS (Figure 2) and contained phagocytic macrophages that release excessive amounts of TNF- α , a proinflammatory cytokine, upon stimulation (Figure 3).

Iron overload polarizes macrophages toward inflammatory M1-like phenotypes,²¹ which can release substantial amounts of proinflammatory cytokines, including TNF- α and interleukin (IL)-6.²² Since long-term treatment with LPS induces M1 macrophage polarization,^{23,24} the excessive release of TNF- α from splenocytes after LPS treatment suggested that M1-like macrophages may abundantly exist in iron-accumulating spleens of TSOD mice. Moreover, inflammatory cytokines trigger the upregulation of *Hamp*, which encodes hepcidin,²⁵ a protein that modulates the cytokine-induced inflammatory response mediated by the upregulation of suppressor of cytokine signaling 3, a negative regulator of JAK/STAT signaling.^{23,26} Hepcidin modulates iron metabolism and cytokine-induced inflammation in coordination with STAT3.^{26,27} Thus, the increased expression of splenic *Hamp* in TSOD mice (Figure 1(d)) may contribute to suppress the excessive and detrimental inflammation induced by M1-like macrophages. In fact, control TSOD cells (without stimulus) did not release TNF- α (Figure 3). However, the activation of splenic macrophages by exposure to LPS (Figure 3), which can occur through the ingestion of contaminated food and gram-negative bacteria, led to high TNF- α release. The production of transforming growth factor (TGF)- β and IL-6 in the spleen may affect liver fibrosis progression in cirrhosis patients via liver-spleen cross-talk.²⁸ It is noteworthy that splenic macrophage-derived leukotriene B4 enhances TNF- α secretion by hepatic Kupffer cells through the portal vein, and that splenectomy inhibits LPS-induced expression of TNF- α in the liver.²⁹ These findings indicate that spleen-derived humoral factors strongly

contribute to the regulation of hepatic inflammation, and that cytokines released by splenic cells may be involved in NASH development.

ROS generation can occur not only through Fe²⁺-mediated Fenton reaction but also through activated macrophages,³⁰ which were abundant in the spleens of TSOD mice. However, ROS generation was only approximately 2-fold higher in the spleens from TSOD mice than in those from TSNO mice, regardless of H₂O₂ exposure (Figure 2(a)), even though the iron level in the spleens from TSOD mice was 20-fold higher than that in those from TSNO mice (Figure 1(a) and (b)). Our findings suggest that the antioxidant capacity in the spleens of TSOD mice exhibiting NASH at an early stage may be enhanced by increasing the gene expression of the antioxidant enzymes *Hmox1* and *Gpx1* (Figure 2(b) and (c)). Indeed, the splenic antioxidant capacity in obese mice has been shown to be higher than that in normal control mice.³¹ Furthermore, the half-life of a hydroxyl radical with a high reactivity is about 10⁻⁹s in cells;³² therefore, the ROS generated in the spleen may be unable to directly induce oxidative damage in the liver. However, intracellular ROS promotes the production of inflammatory cytokines^{33,34} that may lead to hepatic inflammation. Thus, a slight increase in splenic ROS may be involved in the exacerbation of NASH.

In conclusion, we found that iron-accumulating splenocytes generate moderate amounts of ROS and release high amounts of TNF- α after macrophage stimulation. Although a direct involvement of the splenic iron accumulation in NASH was not clarified, we will investigate the effect of splenectomy on the development of NASH in TSOD mice in the next study. Since spleen-derived ROS and inflammatory cytokines may indirectly contribute to hepatic inflammation, the regulation of iron metabolism in the spleen should be considered in the development of novel therapeutic targets against NASH.

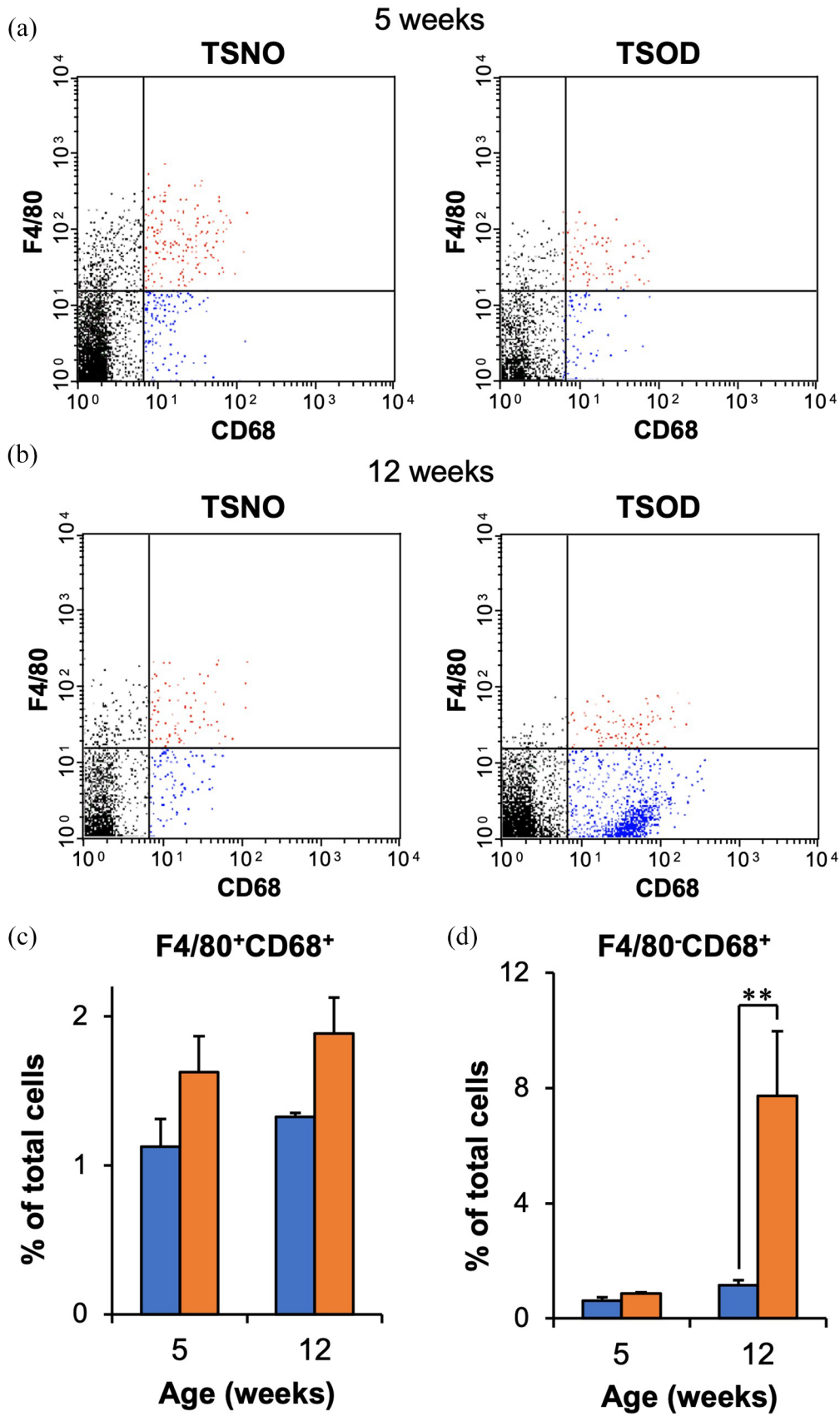


Figure 4. Macrophage subset in the spleens of TSNO and TSOD mice. Representative results of the flow cytometric analysis showing F4/80 and CD68 expression in splenocytes of 5- (a) and 12- (b) week-old TSNO and TSOD mice. Red and blue dots represent F4/80⁺CD68⁺ and F4/80⁻CD68⁺ cells, respectively. The percentage of F4/80⁺CD68⁺ (c) and F4/80⁻CD68⁺ (d) cells in the spleens of 5- and 12- week-old mice.

Data are presented as mean values \pm SE ($n=3$ each).

** $P < 0.01$ compared with TSNO.

AUTHORS' CONTRIBUTIONS

K.M. conceived and designed the study. All authors conducted the experiments and analyzed the data. K.M. and M.Y. wrote and edited the manuscript. All authors approved the final version for submission.


DECLARATION OF CONFLICTING INTERESTS

The author(s) declared no potential conflicts of interest with respect to the research, authorship, and/or publication of this article.

FUNDING

The author(s) disclosed receipt of the following financial support for the research, authorship, and/or publication of this article: This work was supported by the Japan Society for the Promotion of Science KAKENHI (grant no. 19K07057).

ORCID ID

Kazutoshi Murotomi  <https://orcid.org/0000-0002-2124-1538>

REFERENCES

- Peng C, Stewart AG, Woodman OL, Ritchie RH, Qin CX. Non-alcoholic steatohepatitis: a review of its mechanism, models and medical treatments. *Front Pharmacol* 2020;**11**:603926
- Day CP, James OF. Steatohepatitis: a tale of two "hits"? *Gastroenterology* 1998;**114**:842–5
- Buzzetti E, Pinzani M, Tsochatzis EA. The multiple-hit pathogenesis of non-alcoholic fatty liver disease (NAFLD). *Metabolism* 2016;**65**:1038–48
- Manne V, Handa P, Kowdley KV. Pathophysiology of nonalcoholic fatty liver disease/nonalcoholic steatohepatitis. *Clin Liver Dis* 2018;**22**:23–37
- Marra F, Svegliati-Baroni G. Lipotoxicity and the gut-liver axis in NASH pathogenesis. *J Hepatol* 2018;**68**:280–95
- Schuster S, Cabrera D, Arrese M, Feldstein AE. Triggering and resolution of inflammation in NASH. *Nat Rev Gastroenterol Hepatol* 2018;**15**:349–64
- Svegliati-Baroni G, Patricio B, Lioci G, Macedo MP, Gastaldelli A. Gut-pancreas-liver axis as a target for treatment of NAFLD/NASH. *Int J Mol Sci* 2020;**21**:5820
- Li X, Wang H. Multiple organs involved in the pathogenesis of non-alcoholic fatty liver disease. *Cell Biosci* 2020;**10**:140
- Pierantonelli I, Svegliati-Baroni G. Nonalcoholic fatty liver disease: basic pathogenetic mechanisms in the progression from NAFLD to NASH. *Transplantation* 2019;**103**:e1–13
- Aoyama T, Kuwahara-Arai K, Uchiyama A, Kon K, Okubo H, Yamashina S, Ikejima K, Kokubu S, Miyazaki A, Watanabe S. Spleen-derived lipocalin-2 in the portal vein regulates Kupffer cells activation and attenuates the development of liver fibrosis in mice. *Lab Invest* 2017;**97**:890–902
- Zheng Z, Wang H, Li L, Zhang S, Zhang C, Zhang H, Ji F, Liu X, Zhu K, Kong G, Li Z. Splenectomy enhances the Ly6C(low) phenotype in hepatic macrophages by activating the ERK1/2 pathway during liver fibrosis. *Int Immunopharmacol* 2020;**86**:106762
- Oishi T, Terai S, Iwamoto T, Takami T, Yamamoto N, Sakaida I. Splenectomy reduces fibrosis and preneoplastic lesions with increased triglycerides and essential fatty acids in rat liver cirrhosis induced by a choline-deficient L-amino acid-defined diet. *Hepatol Res* 2011;**41**:463–74
- Nishida T, Tsuneyama K, Fujimoto M, Nomoto K, Hayashi S, Miwa S, Nakajima T, Nakanishi Y, Sasaki Y, Suzuki W, Iizuka S, Nagata M, Shimada T, Aburada M, Shimada Y, Imura J. Spontaneous onset of nonalcoholic steatohepatitis and hepatocellular carcinoma in a mouse model of metabolic syndrome. *Lab Invest* 2013;**93**:230–41
- Murotomi K, Arai S, Uchida S, Endo S, Mitsuzumi H, Tabei Y, Yoshida Y, Nakajima Y. Involvement of splenic iron accumulation in the development of nonalcoholic steatohepatitis in Tsumura Suzuki Obese Diabetes mice. *Sci Rep* 2016;**6**:22476
- Ganz T, Nemeth E. Hepcidin and iron homeostasis. *Biochim Biophys Acta* 2012;**1823**:1434–43
- Franco AA, Odom RS, Rando TA. Regulation of antioxidant enzyme gene expression in response to oxidative stress and during differentiation of mouse skeletal muscle. *Free Radic Biol Med* 1999;**27**:1122–32
- Wang Z, Yin W, Zhu L, Li J, Yao Y, Chen F, Sun M, Zhang J, Shen N, Song Y, Chang X. Iron drives T helper cell pathogenicity by promoting RNA-binding protein PCBP1-mediated proinflammatory cytokine production. *Immunity* 2018;**49**:80–92.e7
- Borges da Silva H, Fonseca R, Pereira RM, Cassado Ados A, Alvarez JM, D'Imperio Lima MR. Splenic macrophage subsets and their function during blood-borne infections. *Front Immunol* 2015;**6**:480
- Leenen PJ, de Bruijn MF, Voerman JS, Campbell PA, van Ewijk W. Markers of mouse macrophage development detected by monoclonal antibodies. *J Immunol Methods* 1994;**174**:5–19
- Dambach DM, Watson LM, Gray KR, Durham SK, Laskin DL. Role of CCR2 in macrophage migration into the liver during acetaminophen-induced hepatotoxicity in the mouse. *Hepatology* 2002;**35**:1093–103
- Zhou Y, Que KT, Zhang Z, Yi ZJ, Zhao PX, You Y, Gong JP, Liu ZJ. Iron overloaded polarizes macrophage to proinflammation phenotype through ROS/acetyl-p53 pathway. *Cancer Med* 2018;**7**:4012–22
- Vogel DY, Heijnen PD, Breur M, de Vries HE, Tool AT, Amor S, Dijkstra CD. Macrophages migrate in an activation-dependent manner to chemokines involved in neuroinflammation. *J Neuroinflammation* 2014;**11**:23
- Qin H, Holdbrooks AT, Liu Y, Reynolds SL, Yanagisawa LL, Benveniste EN. SOCS3 deficiency promotes M1 macrophage polarization and inflammation. *J Immunol* 2012;**189**:3439–48
- Zhang W, Zhang YT, He YX, Wang XY, Fang Q. Lipopolysaccharide mediates time-dependent macrophage M1/M2 polarization through the Tim-3/Galectin-9 signalling pathway. *Exp Cell Res* 2019;**376**:124–32
- Lee P, Peng H, Gelbart T, Wang L, Beutler E. Regulation of hepcidin transcription by interleukin-1 and interleukin-6. *Proc Natl Acad Sci USA* 2005;**102**:1906–10
- De Domenico I, Zhang TY, Koenig CL, Branch RW, London N, Lo E, Daynes RA, Kushner JP, Li D, Ward DM, Kaplan J. Hepcidin mediates transcriptional changes that modulate acute cytokine-induced inflammatory responses in mice. *J Clin Invest* 2010;**120**:2395–405
- Maliken BD, Nelson JE, Kowdley KV. The hepcidin circuits act: balancing iron and inflammation. *Hepatology* 2011;**53**:1764–6
- Asanoma M, Ikemoto T, Mori H, Utsunomiya T, Imura S, Morine Y, Iwahashi S, Saito Y, Yamada S, Shimada M. Cytokine expression in spleen affects progression of liver cirrhosis through liver-spleen crosstalk. *Hepatol Res* 2014;**44**:1217–23
- Fonseca MT, Moretti EH, Marques LMM, Machado BF, Brito CF, Guedes JT, Komegae EN, Vieira TS, Festuccia WT, Lopes NP, Steiner AA. A leukotriene-dependent spleen-liver axis drives TNF production in systemic inflammation. *Sci Signal* 2021;**14**:eabb0969
- Bae YS, Lee JH, Choi SH, Kim S, Almazan F, Witztum JL, Miller YI. Macrophages generate reactive oxygen species in response to minimally oxidized low-density lipoprotein: toll-like receptor 4- and spleen tyrosine kinase-dependent activation of NADPH oxidase 2. *Circ Res* 2009;**104**:210–8, 21p following 18
- Gu X, Ma Z, Fang J, Cai D, Zuo Z, Liang S, Cui H, Deng J, Ma X, Ren Z, Geng Y, Zhang M, Ye G, Xie Y, Gou L, Hu Y. Obesity enhances antioxidant capacity and reduces cytokine levels of the spleen in mice to resist splenic injury challenged by *Escherichia coli*. *J Immunol Res* 2020;**2020**:5948256
- D'Autreaux B, Toledano MB. ROS as signalling molecules: mechanisms that generate specificity in ROS homeostasis. *Nat Rev Mol Cell Biol* 2007;**8**:813–24
- Mittal M, Siddiqui MR, Tran K, Reddy SP, Malik AB. Reactive oxygen species in inflammation and tissue injury. *Antioxid Redox Signal* 2014;**20**:1126–67
- Kim YH, Kumar A, Chang CH, Pyaram K. Reactive oxygen species regulate the inflammatory function of NKT cells through promyelocytic leukemia zinc finger. *J Immunol* 2017;**199**:3478–87

(Received October 7, 2021, Accepted January 12, 2022)